CHAPTER THREE

DECAY LAW MODELLING AND ESTIMATES OF SOURCE PARAMETERS FROM SEISMIC AMPLITUDE

3.1 Introduction

There are many issues which must be considered in order to model volcano-seismic wavefields, even if homogeneous media are assumed. At volcanoes, near field effects cannot be ignored, especially for long period waves. In addition there are effects at the free surface and sources of noise which greatly modify the waveforms recorded.

By taking account of some of these issues simple models are derived for a point line and a (finite) line source, in order that pressure changes can be estimated for the underlying phase associated with eruptions at vent 1 of Stromboli. In particular, both near and far field terms are included and weighted according to the wavelength of the signal recorded. A trade-off is found between source volume and pressure making it impossible to determine one parameter without an estimate of the other. Therefore a range of source radii from 1 to 100 m is used. Small radii sources are ruled out because strains become very large. In addition, the Bernoulli effect can be eliminated as a significant generator of seismic signals because required mass fluxes are several orders of magnitude larger than those observed.

Other source types of relevance to volcano seismology are then discussed, in addition to (stationary) point sources and line sources. New types of sources identified in this thesis are the moving point source, and the expanding line source, neither of which have been discussed in relation to volcano-seismic sources before. Examples of the processes that might result in each source type are provided. All the work in the chapter is original.

3.2 How a signal is generated

What does a seismogram tell us? Can it be interpreted as a record of pressure changes within the volcano? That would be very convenient and is an assumption that many are quick to make, but it has its pitfalls. As wavefronts travel from source to seismometer they are subject to all the phenomena of wave propagation: refraction, reflection, diffraction and dispersion. Even if the solid is assumed to be homogenous there are still reflections and mode conversions at boundaries to contend with. And even if these are negligible, there are further complications:

- The source itself may not be a simple point source. Instead it may be moving, and the source region itself may be extended – for example the pressure could be changing throughout the entire conduit.

- The waveform recorded in the near field is more complicated than that recorded in the far field, because it contains terms where P and S waves cannot be separated [e.g. *Aki and Richards*, 1980].

- There are several sources of noise, particularly ocean microseisms with periods as low as 10 s, and wind noise which has a broadband signal.

For these reasons it is necessary to go back to basics and consider each part of the propagation problem separately.

Consider the simple model depicted in Fig. 3.1. Fluid pressure changes alter the boundary conditions at the conduit wall, leading to the generation of seismic waves which propagate through many layers of volcanic rock and ash. They interact with the free surface and are recorded by a seismometer. So there are 5 parts to the problem: two media (fluid and solid), two interfaces (conduit wall and free surface) plus a seismometer. Each medium or interface can be thought of as a filter that alters the signal. (For simplicity all media are assumed to be homogeneous and isotropic. This is normally justified because only long wavelengths are of interest).

(a)

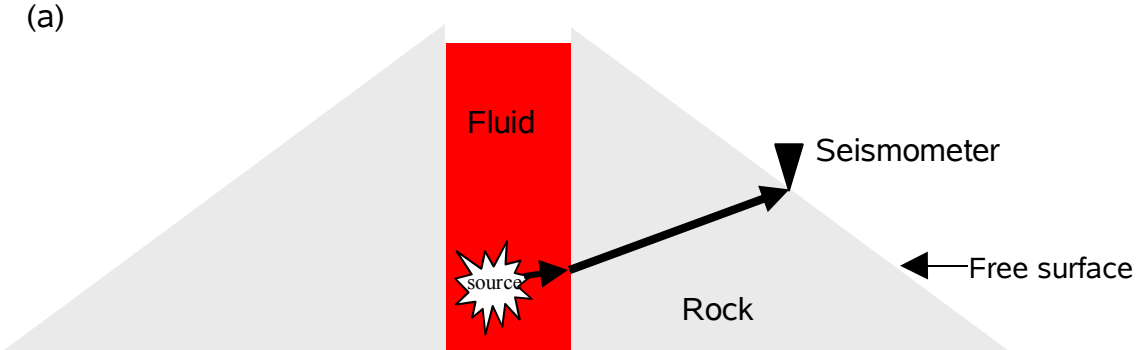

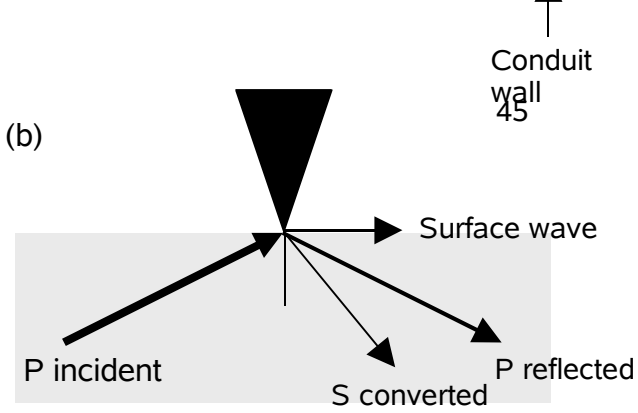

Figure 3.1: (a) A sharp pressure change acts as a source of pressure waves in the fluid (magma). These waves generate P and S waves at the conduit wall which propagate through the solid (layers of lava and ash). These seismic waves interact with the free surface (b) to produce reflections and mode conversions. The ground motion detected by the seismometer is the vector sum of all these waves.

In order to generate a seismic signal, some pressure change must occur within the magmatic system, perhaps in response to exsolution caused by steady (aseismic) magma rise. This leads to a pressure/stress discontinuity at the conduit/magma chamber wall. Particles in rock adjacent to the conduit wall now move in response to this stress difference, but as a result they are no longer at a stable distance from neighboring particles in the solid, so those particles move too. The neighbors of those particles are then caused to react, and so on. On the macroscopic level an elastic seismic wave is observed, propagating outward from the source, diminishing in amplitude as the wavefront spreads out, and as energy is dissipated in other forms.

When these elastic waves interact with the free surface, new waves are produced. The seismometer, which is at the free surface, picks up the incoming seismic wave at exactly the moment these new wave types are produced, and so records the vector sum of all the waves (the boundary conditions are matched). This is why the 'surface correction' of *Neuberg and Luckett* [1996] is needed to resolve the

polarization of the incoming wave, and hence to determine the seismic source location by back-projection of the incident P wave.

Finally, the seismometer cannot have a perfect response at all frequencies, so it is necessary to deconvolve the impulse response of the instrument from the recorded seismogram in order to estimate the true ground motion.

3.2.1 Fluid

In the following paragraphs, the aim is to summarise how physical parameters of the fluid change as it rises up the conduit. The most important physical parameter of the magma is its viscosity, which determines to a large degree the type of activity that can occur. Other important parameters are pressure, density and rise speed.

Viscosity increases as the flow rises because water exsolves as the pressure drops. Increased viscosity inhibits bubble growth, leading to increased overpressure (and a tendency towards more explosive eruptions). As overpressure increases, magmatic pressure deviates more and more from the lithostatic gradient, hence the pressure gradient mirrors the viscosity profile. Indeed, in order for magma to rise, the pressure difference over an element of the flow must exceed the viscous drag forces [Fig. 3.2]. However, for low viscosity basaltic magmas, which usually lead to Hawaiian or Strombolian activity, these deviations are small.

Density of the flow decreases as bubbles grow. At depth the density is close to the density of the surrounding rock, but decreases as the relative bubble volume increases due to decompression as the magma rises. For Stromboli the relative bubble probably never exceeds 75% since that is believed to lead to fragmentation, a process characteristic of Plinian activity and not observed normally at Stromboli. If true, the density of the two-phase fluid at Stromboli would be at least one-quarter of rock density, and probably much higher.

Temperature hardly changes. Magma takes of the order of 1 hour to rise from the chamber to the surface, which is insufficient for it to cool much [*Dehn, J.*, Alaska Volcano Observatory, pers. comm., March 1999].

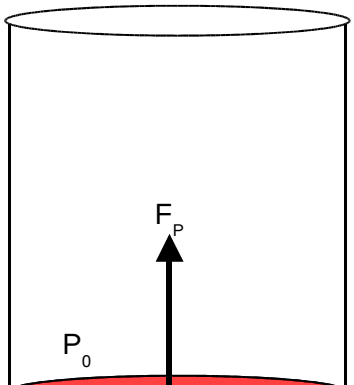

A = cross sectional area

F_P = pressure force = $(P_1 - P_0)\,A$

F_D = viscous drag force

W = weight of element = $\rho\, A\, \delta z\, g$

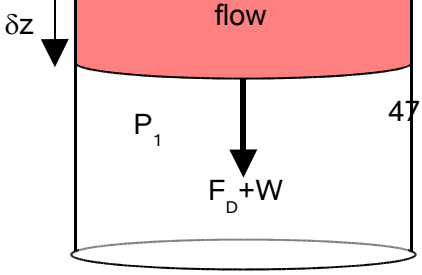

Figure 3.2: In order for magma to rise a pressure gradient must exist. This must provide sufficient upward directed pressure force to overcome the weight of the element and viscous drag forces.

Is it necessary to consider viscous effects at all for Stromboli? The Reynolds number can be used to assess whether it is necessary to include viscous effects in the modelling process. It is given by:

$$R = \frac{UL\rho}{\eta} \qquad \textbf{(3-1)}$$

where U is the characteristic speed of the flow, L is the characteristic length, ρ is density and η is viscosity. R<<1700 indicates laminar flow in which case viscous terms are important, whereas R>>1700 indicates turbulent flow [*Tritton*, 1988].

For activity at Stromboli, reasonable physical parameters are U=0.1 m/s, L=400 m, ρ=2000 kg/m^3 and η=1000 Pa s [e.g. *Parfitt and Wilson*, 1995]. This gives R=80, indicating that viscosity cannot be ignored.

To analyse the waves propagating within the fluid, the relation between stress and strain or strain rate in the fluid needs to be modelled. For a Newtonian fluid, stress is proportional to strain rate [e.g. *Tritton*, 1988]. For a solid, stress is proportional to strain (Hooke's law). These complications can be ignored since the aim in this

chapter is to calculate average pressure in the conduit, not analyse seismic waves propagating in the conduit.

3.2.2 Conduit wall

This is the interface between a fluid and a solid. Assuming a cylindrical conduit partially filled with viscous magma, radial and vertical displacement must be continuous (no slip). Radial and shear stress components must also be continuous (think of thin layers). If the fluid were inviscid, slip would occur and shear stress would be zero at conduit wall. Different boundary conditions lead to different wavefields in the solid.

3.2.3 Solid

Providing the fluctuations in stress are small the rock will not be strained beyond its elastic limit and so the solid behaves elastically. If the rock is not strained beyond its limit of proportionality, Hooke's law will hold. Furthermore, the rock can be assumed to be homogeneous and isotropic if the waves of interest have wavelengths that are greater than the largest material inhomogeneities present within the volcanic structure. Refraction and diffraction only becomes important the conduit wall or free surface.

3.2.4 Free surface

Three things happen when a wavefront encounters any boundary:

- energy is partially reflected in the form of a P and an S wave
- energy is partially transmitted / refracted,
- interface waves are produced.

The amplitude ratios of these various waves are given by Knott's equations or Zoeppritz's equations [e.g. *Sheriff and Geldart*,1995].

At the free surface the impedance contrast is particularly large, leading to strong reflected waves and surface waves (negligible energy is transmitted into the air). The seismometer of course responds to the movement of the free surface: it not

only records the motion caused by the incident body wave, it records the vector sum of many different waves [Fig. 3.1b]. *Neuberg and Pointer* [1999] describe a *surface correction* which can be used to recover the original polarization of the incident body wave.

Topographic features which are comparable in size to seismic wavelengths cause scattering leading a noisy seismogram. This surface wave noise affects short-period signals more than VLP signals since few features are large enough to scatter VLP waves. *Luckett* [1997] found site-dependent peaks in tremor spectra from Stromboli. Polarization analysis of eruptive events at Stromboli shows that a deeper source is indicated for lower filter bands, indicating that higher frequencies are heavily contaminated by topographic scattering / site effects. Coherency is better for the lower frequencies. These are more reasons for using broadband rather than short-period seismometers.

3.2.5 Seismometer

The seismometer cannot respond equally at all frequencies. Each seismometer has a unique transfer function which must be deconvolved from the signal to recover true ground motion. The transfer function can be found by measuring the response of the seismometer to purely sinusoidal waves of many different frequencies on a shake table, or the response to a delta pulse.

Seismometers are designed to work with their base aligned horizontally. Seismometers deployed at the summit or on the flanks of a volcano will deviate from this alignment as the volcano swells and deflates due to movements of magma and pressurisation within. This 'tilting' effect is particularly important for the horizontal components of a seismometer because it is proportional to the sine of the tilt angle [Section 2.4.3]. The importance of tilting also depends on frequency (worse for low frequencies because it is necessary to integrate to get displacement). The effect of tilt on long-period signals at Stromboli has been studied by *Forbriger and Wielandt* [1997].

If the seismometer does not have good contact with the ground then a poor representation of ground motion is produced. It is therefore best sited on solid rock (although in a volcanic environment, this quite often sits on very loose material).

In addition there is noise. There are several causes of this:

- There is background white noise, dependent on the temperature of the electronics. This is why astronomers cool their CCD cameras prior to recording an image. For seismology the signal to noise ratio is a lot better so cooling would be of no benefit.

- Noise from electric currents in the ground and magnetic fields as a result of power cables. This is why when installing seismic cables have to be fixed in position. If the cable moves (due to the wind) it will induce a current (Faraday's law) since it is a conductor moving in a magnetic field.

- Environmental noise due to wind, rain, lightning, variations in temperature, groundwater movement, traffic and other cultural noise.

For the purposes of this work some types of seismicity are also considered to be noise, because they are unrelated to movements within the magmatic system. Among these are tectonic earthquakes (including a-type events), landslides, rockfalls, pyroclastic flows, lahars, ocean microseism and movements of groundwater and glacial melt.

3.2.6 Near field

When the elasto-dynamic wave equation is solved there are additional terms which can be conveniently ignored in global and exploration seismology [e.g. *Aki and Richards*, 1980]. These are the near field terms, so called because they dominate seismograms for stations which are very close to the source. This happens because these terms decay more rapidly with distance than do the far field terms.

Aki and Richards [1980] define the near field as the region that lies within one wavelength of the source. Notice the definition of the near field has nothing to do with the size of the source region: a seismometer can be in the near field of a point source.

In volcano seismology it is crucial to consider near field effects as seismometers are frequently deployed within one seismic wavelength of the source. This is particularly the case for VLP signals at Stromboli which have wavelengths of up to 28 km. Ignoring near field terms can lead to an estimate of source pressure which is more than an order of magnitude too small [Section 3.3].

VLP	SP

• Near field effects must be considered • Reasonable to treat media as homogeneous and isotropic – negligible scattering • Surface waves are not as important • Tilt-induced signals likely to be significant on horizontal components • Attenuation is negligible	• Near field effects may be negligible especially at higher frequencies or furthest stations • Anisotropy is probably significant – waves are scattered • Surface waves may dominate signal and lead to an estimate of source depth which is too shallow • Tilt-induced signals are negligible • Attenuation may be important at higher frequencies or furthest stations

Table 3.1: Different points to be considered when modelling very long period (VLP, 2-20 s) signals, when compared to short period (SP, 0.5-10 Hz) signals. This summarises some of the points made in Section 3.2. Regardless of signal type, modelling must consider the effects of a viscous fluid.

3.3 Decay law modelling method

3.3.1 Introduction

In this section a new modelling method will be derived, the aim of is to infer the size of pressure changes within the conduit system at Stromboli from the amplitude of the seismic signals observed. There are two parts to the problem: first an expression relating particle displacement at the source boundary to the magnitude of fluid pressure change within the source region is derived. Secondly a method for extrapolating displacement at the source boundary from that recorded at the seismometer is found. This part is done using decay laws, which express how seismic displacement decreases (decays) with increasing distance from the source. For this reason the method is called the 'decay law method'. Separate models are developed for a point source and a line source.

The assumptions of these models are as follows, based on Section 3.2:

- All media are homogeneous and isotropic (a reasonable assumption at VLP wavelengths since stations are well within a wavelength of the source),
- The fluid in the conduit (magma & gas mixture) is inviscid, therefore the stress in all directions is equal to fluid pressure,
- Attenuation, other than by geometrical spreading, is negligible (very reasonable in the near field),
- There are no reflections or mode conversions at the free surface,
- Seismic waves in the solid are generated by changes in fluid pressure.

3.3.2 Pressure and volume changes for a point source

Consider a model consisting of a spherical, fluid-filled, magma chamber of radius r_0. The following is developed in spherical co-ordinates to take advantage of symmetry. Continuity of radial stress between the fluid and solid implies:

$$\sigma_{rr}(r_0) = -\Delta P \qquad \textbf{(3-2)}$$

where σ_{rr} is the change in radial stress in the solid corresponding to a change, ΔP, in the fluid pressure. The stress for a spherically symmetric source with no SH waves is:

$$\sigma_{rr}(r_0) = \lambda\left(u_{r:r}(r_0) + 2\frac{u_r(r_0)}{r_0}\right) + 2\mu u_{r:r}(r_0) \qquad \textbf{(3-3)}$$

Where subscripts following a colon are used to denote differentiation, hence du_r/dr is represented by $u_{r:r}$. Eliminating elastic constants λ and μ in favour of P wave speed, α, and S wave speed, β, gives:

$$-\Delta P = \rho\alpha^2 u_{r:r}(r_0) + 2\rho(\alpha^2 - 2\beta^2)\frac{u_r(r_0)}{r_0}. \qquad \textbf{(3-4)}$$

Given $u_r(r_0)$ it is possible estimate ΔP using 3-4, if required, ΔV can be calculated from 3-5. The remaining problem then is to estimate $u_r(r_0)$ and $u_{r:r}(r_0)$ given $u_r(r_s)$, which is the radial displacement recorded at a station a distance r_s from the source. This problem will be addressed in section 3.3.4.

An aside: If the displacement at $r=r_0$ is $u_r(r_0)$, then the overall volume change, ΔV, of the spherical magma body is:

$$\Delta V = \frac{4}{3}\pi\left[(r_0 + u_r)^3 - r_0^3\right] \qquad \textbf{(3-5)}$$

where V_0 is the volume of the magma body prior to the pressure rise.

3.3.3 Pressure and volume changes for a line source

The above analysis is now performed for a (finite) line source, instead of a point source. Consider a model consisting of a vertical, fluid-filled, cylindrical conduit, radius r. There must be continuity of normal stress at the conduit wall which implies:

$$\sigma_{rr}(r_0) = -\Delta P \qquad \textbf{(3-6)}$$

where σ_{rr} is the radial stress in the solid and ΔP is the fluid pressure. The stress in cylindrical co-ordinates for an axially symmetric source with no SH waves is:

$$\sigma_{rr}(r_0) = \lambda\left(u_{r:r}(r_0) + \frac{u_r(r_0)}{r_0}\right) + 2\mu u_{r:r}(r_0) \qquad \textbf{(3-7)}$$

Then eliminating elastic constants in favour of P wave speed and S wave speed yields:

$$-\Delta P = \rho\alpha^2 u_{r:r}(r_0) + \rho\left(\alpha^2 - 2\beta^2\right)\frac{u_r(r_0)}{r_0}. \qquad \textbf{(3-8)}$$

Again, the problem is to find a method for estimating $u_r(r_0)$ given $u_r(r_s)$.

Although the formulae for point sources and line sources are remarkably similar (compare 3-4 and 3-8) it must be remembered that *r* has different meanings in spherical and cylindrical coordinates.

3.3.4 Decay law modelling

The displacement recorded at a particular distance from a point source involves both near and far field terms. It is often necessary to determine which of these terms dominates in order to proceed with modelling. For example, *Luckett* [1997] presents a graph of radial displacement versus differential travel-times for one event recorded at 9 broadband stations at Stromboli in 1992. He then attempts to fit a near field decay law, and then a far field decay law, in order to determine which of them best fits the data. His overall goal was to determine when the seismic waves were produced at the source.

Another example is from the *reduced displacement* formulation employed at the Alaska Volcano Observatory. This is a correction for geometrical spreading and is employed in an attempt to recover the displacement recorded at a fixed distance from the source [e.g. *Aki and Koyanagi*, 1981]. Reduced displacements for different volcanoes can be meaningfully compared. Again tests were made to see whether the near field or far field term dominates, because they need correcting for in different ways.

The point is that displacement is always a mixture of near and far field terms, so shouldn't models include both? This has not been attempted previously, and it may not be trivial. The plausibility of including both near and far field effects in the modelling will now be considered.

In order to demonstrate the manner in which displacement decays with distance, decay law graphs are plotted. These are plots of how rapidly seismic displacement is decaying with distance at any particular distance. For example if displacement is given by:

$$u(r) = \frac{k}{r^{p}} \qquad \textbf{(3-9)}$$

Then a decay law graph is a plot of *p(r)* versus *r*. In the following the parameter *p(r)* is referred to as 'the power of the decay law'. If only the near field (or the far field)

term is considered, *p* is constant. However if both terms are modelled, *p(r)* will vary, and will generally have a non-integer value.

In order to calculate *p(r)*, consider the displacement at points a small distance δr either side of *r*:

$$u(r-\delta r)=\frac{k}{(r-\delta r)^{p}} \qquad \textbf{(3-10)}$$

and:

$$u(r+\delta r)=\frac{k}{(r+\delta r)^{p}} \qquad \textbf{(3-11)}$$

Combining these and rearranging for *p(r)* gives:

$$p(r)=\lim_{\delta r\to 0}\left(\frac{\log\left(\frac{u(r-\delta r)}{u(r+\delta r)}\right)}{\log\left(\frac{r+\delta r}{r-\delta r}\right)}\right). \qquad \textbf{(3-12)}$$

In summary, waves do not generally decay in amplitude like *1/r* or $1/r^2$, because they contain a mixture of near *and* far field terms. The effective decay law can be calculated at any distance by using 3-12, though this has limited applicability to real data since two stations need to be close (δr < 0.1 *r*) and site effects need to be negligible (or equal) at both sites. However, it is a simple matter to compute the expected decay laws (graphs of *p(r)* calculated for a range of *r*), for point sources and line sources, and this is done in the following sections.

3.3.5 Decay laws for a point source

At any particular distance, *r*, from a point source, the displacement of a spherical wave is given by a combination of near and far field terms:

$$u(r) = \frac{n}{r^2} + \frac{f}{r} \equiv \frac{k}{r^p} \qquad \textbf{(3-13)}$$

where *n* and *f* are constants which give the weighting of the near and far field terms respectively. Decay laws [Fig. 3.3] were calculated using the method described in the previous section. Sufficiently close to the source, $p(r) \cong 2$, since the near field term dominates. Far from the source $p(r) \cong 1$, since the far field term dominates.

However, the interesting result is that when the decay law is plotted for different values of *n/f*, $p(r) = 1.5$ always corresponds to $r = n/f$ (this can be proved algebraically). Analysis of 3-12 in conjunction with 3-13 shows that near and far field terms are equal for $p(r) = 1.5$. One is therefore entitled to define the near field as the range of *r* for which $p(r) > 1.5$, because for these values, the near field term dominates.

The definition of the near field used by *Aki and Richards* [1980] is $r<\lambda$, where λ is the wavelength of the source. Hence the ratio *n/f* is equal to the wavelength of the source, λ, and so 3-13 becomes:

$$u(r) = f\left(\frac{\lambda}{r^2} + \frac{1}{r}\right) \qquad \textbf{(3-14)}$$

This is now a much more useful formula for modelling purposes. The term *f* is an unknown constant (at least for a given wavelength). However, $u(r)$ and λ can be measured from a seismogram (if wave speed is known), and combining these with *r* yields *f*. If there is no particular dominant frequency present in the source, 3-14 can be integrated over a range of wavelengths. Indeed $f(\lambda)$ could be chosen to match the source spectrum.

Figure 3.3

Armed with this better method of estimating $u(r_0)$, the aim is to estimate pressure change, ΔP, using 3-4:

$$-\Delta P = \rho\alpha^2 u_{r;r}(r_0) + 2\rho(\alpha^2 - 2\beta^2)\frac{u_r(r_0)}{r_0}$$

where from 3-14 radial strain is given by:

$$u_{r;r}(r) = -f\left(\frac{2\lambda}{r^3} + \frac{1}{r^2}\right) \quad \textbf{(3-15)}$$

3.3.6 Decay laws for a line source

The point source problem is trivial by comparison to the line source problem. First a line source must be approximated by integrating the formula for a point source between over the length of the conduit [Fig. 3.4]:

The radial component of displacement, $u_r(r,z)$ is given by:

$$u_r(r, z_S) = \frac{f}{z_T - z_B}\int_{z_B - z_S}^{z_T - z_S}\left(\frac{\lambda}{R^2} + \frac{1}{R}\right)\cos\theta\, ds \quad \textbf{(3-16)}$$

The vertical component of displacement, $u_z(r,z)$ is given by:

$$u_z(r, z_S) = \frac{f}{z_T - z_B}\int_{z_B - z_S}^{z_T - z_S}\left(\frac{\lambda}{R^2} + \frac{1}{R}\right)\sin\theta\, ds \quad \textbf{(3-17)}$$

Using the following integrals:

$$\int\frac{\cos\theta}{R}ds = \int\frac{r}{r^2 + s^2}ds = \tan^{-1}{}^{s}\!\!\diagup\!\!_{r} \quad \textbf{(3-18)}$$

$$\int\frac{\sin\theta}{R}ds = \int\frac{s}{r^2 + s^2}ds = \frac{1}{2}\ln\left(r^2 + s^2\right) \quad \textbf{(3-19)}$$

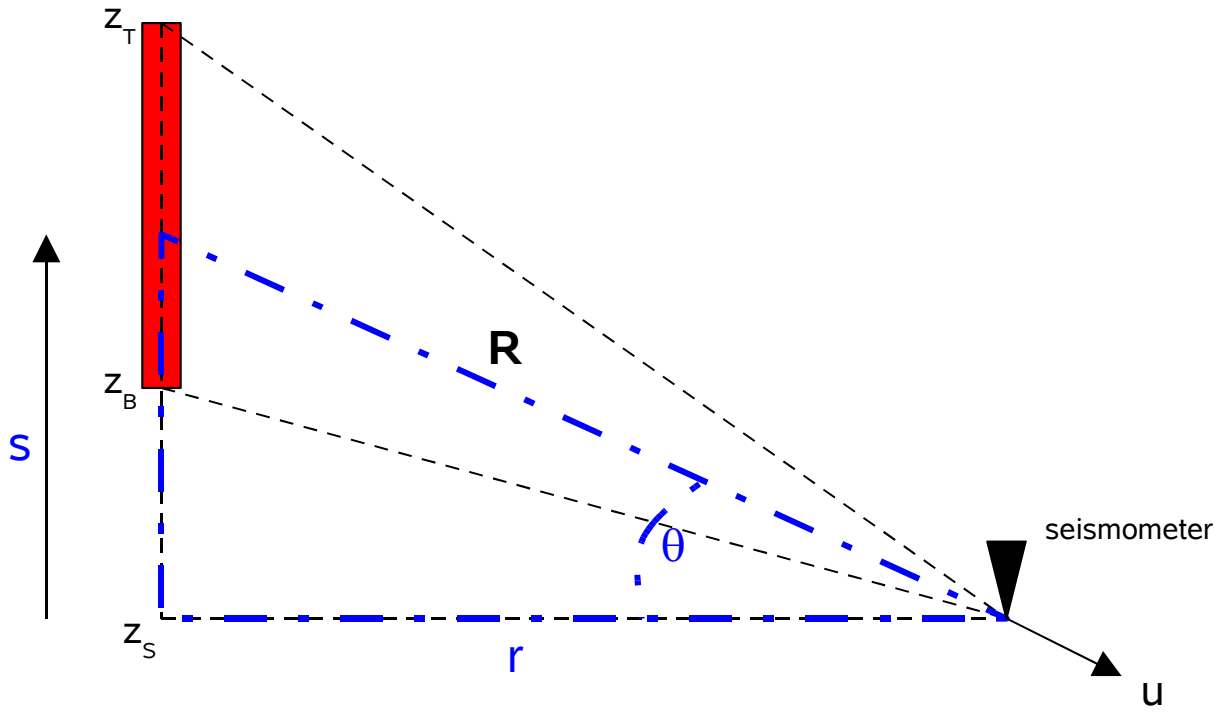

Figure 3.4: A line source (red box) is approximated by integrating the point source formula (3-14) from $s=z_B-z_S$ to $s=z_T-z_S$.

$$\int \frac{\lambda}{r^2}\cos\theta\, ds = \int \frac{\lambda}{r}\cos\theta\, d\theta = \frac{\lambda}{r}\sin\theta \qquad \textbf{(3-20)}$$

$$\int \frac{\lambda}{r^2}\sin\theta\, ds = \int \frac{\lambda}{r}sion\,\theta\, d\theta = -\frac{\lambda}{r}\cos\theta \qquad \textbf{(3-21)}$$

where in 3-20 and 3-21 the result $\frac{ds}{R^2} = \frac{d\theta}{r}$ is used, equations 3-16 and 3-17 reduce to:

$$u_z(r, z_S) = \frac{f}{z_T - z_B}\left[\frac{\lambda}{r}\left(\sin\theta_T - \sin\theta_B\right) + \left(\theta_T - \theta_B\right)\right] \qquad \textbf{(3-22)}$$

and

$$u_z(r, z_S) = \frac{f}{z_T - z_B}\left[\frac{1}{2}\ln\left\{\frac{r^2 + \left(z_T^2 - z_S^2\right)}{r^2 + \left(z_B^2 - z_S^2\right)}\right\} - \frac{\lambda}{r}\left(\cos\theta_T - \cos\theta_B\right)\right]. \qquad \textbf{(3-23)}$$

The resulting decay laws for a line source are intriguing [Fig. 3.5]. There are two factors at play here:

1. Near field dominates for $\lambda<r$, far field for $\lambda>r$. These terms are shown separately in Fig. 3.6a.

2. As *r* increases, the line source subtends a smaller angle, so it behaves more and more like a point source. This transition occurs around $r=L/2$ [Fig. 3.6b].

Hence for $\lambda<L/2$, *p(r)* dips below 1, because the far field term starts to dominate, before the line source has become pointlike.

However for $\lambda>L/2$, *p(r)* is always greater than 1, and approaches 2 as the line source becomes more and more pointlike, before returning to 1 as the near field term becomes negligible.

All curves start and end with $p(r)=1$, because for very small *r* the near field for a line source dominates, and for very large *r*, the far field for a point source dominates.

Now a better method for calculating the displacement from a line source has been found, the parameters estimated in section 3.3.3 can be better constrained by using 3-8:

$$-\Delta P = \rho\alpha^2 u_{r;r}(r_0) + \rho\left(\alpha^2 - 2\beta^2\right)\frac{u_r(r_0)}{r_0}.$$

Radial strain, $u_{r;r}$, can be calculated by differentiating 3-22 with respect to *r,* or by calculating u_r at two close together points.

This completes the derivations for estimating pressure changes for both point sources and finite line source. In the following section, the results of this study are presented.

FIGURE 3.5

Decay laws for a line source

FIGURE 3.6

Line source

(a) near field / far field

(b) source length

3.3.7 Results of simple modelling

The source of the underlying phase corresponding to vent 1 eruptions at Stromboli was investigated. This has a period of 16 s, and a maximum amplitude of ~20 μm at station 197. Two sets of models were performed: in the first the source was assumed to be a point source 350 m below the vents, and in the second the source was assumed to be a line source, with a length of 700 m, oriented vertically. Source radius was the only parameter varied during each set of models, because this is the most critical parameter; this was varied in the range 1-100 m.

Many models can be eliminated because they predict radial strains or pressure changes [Fig. 3.7] which seem to be unrealistic for a volcano like Stromboli, which is very stable and only rarely shows seismo-tectonic activity indicative of rock fracture. Sustained strains of more than ~10^{-5} lead to rock failure [*McNutt*, *S.,* Alaska Volcano Observatory, pers. comm., April 1999], however it is possible that much larger transient strains could occur without leading to rock failure. However, it seems unlikely that transient radial strains of more than about 10^{-3} could be sustained. This corresponds to a line source with a radius of at least 4 m or a point source with a radius of at least 40 m [Fig. 3.7a]. A radial strain of 10^{-3} corresponds to a pressure change of 3 MPa for a line source of radius 4 m, or 4 MPa for a point source of radius 40 m. Although the south-west vent at Stromboli (vent 1) has a radius of about 1 m, it is likely that this widens with depth [*Wilson*, *L.,* Lancaster University, pers. comm., September 1997], as indicated by these results.

The pressure changes indicated by modelling are indeed large. An important consideration is how sensitive these results are to a period of 16 s. To check this, models were run for a range of periods from 0.01 – 100 s, with the aim of calculating the displacement at the conduit wall [Fig. 3.8]. As the period (and therefore wavelength) increases, near field terms become more and more important [equation 3-14] and approaches an upper bound. For a point source [Fig. 3.8a], the displacement is within 10% of this upper bound for periods greater than about 5 s. For a line source [Fig. 3.8b] this 10% difference corresponds to periods greater than about 2 s. The overall conclusion is that the results reported in the previous paragraph hold to within 10% if the period of the VLP phase is at least 5 s.

Figure 3.7

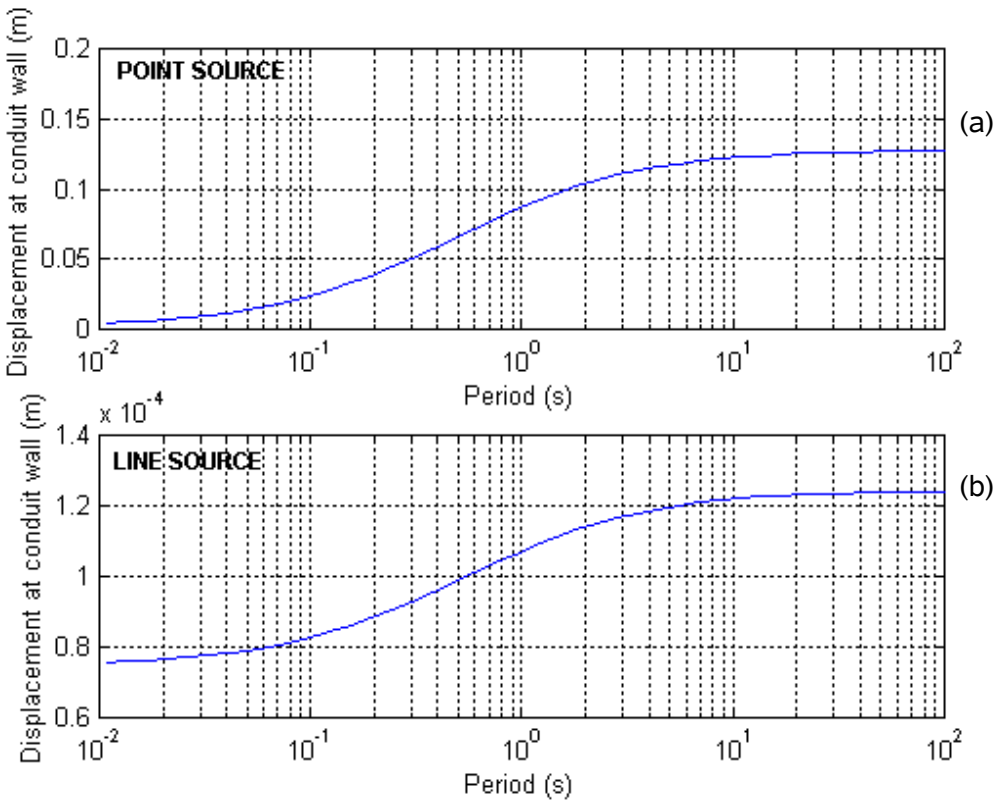

Figure 3.8: Sensitivity to period of the seismic wave. Assuming a conduit radius of 10 m, displacement at the conduit wall was calculated for (a) a point source and (b) a line source, for a range of periods from 0.01 – 100 s. Line source results are very stable, and point source results stable at periods greater than about 3 s.

Neuberg et al. [1994] suggested that the rapid contraction indicated by the underlying phase may be due to the dynamic pressure arising when fluid is accelerated. This is in accordance with Bernoulli's equation:

$$P_d = -\frac{1}{2}\rho v^2 \quad \textbf{(3-24)}$$

This suggests that the pressure in the conduit drops by an amount P_d when the fluid (gas or magma) is accelerated from rest to a speed, v. Assuming that the pressure

changes shown in Fig. 3.7b were produced by this process, *v* was estimated [Fig. 3.9a]. The results (calculated for magma with a density of 2500 kg/m^3) show speeds in the range 2-200 m/s for a line source and 20-10000 m/s. Even gas (which has a much lower density) barely exceeds speeds of 100 m/s during these eruptions [*Ripepe et al.,* 1993] and magma rise speeds probably don't exceed 1 m/s.

Next, consider mass flux, *Q*, where:

$$Q = \rho A v \qquad \textbf{(3-25)}$$

Experimental evidence suggests that during eruptions mass flux (Q) peaks at a few hundred kilograms per second. However, in order for the Bernoulli effect to produce the underlying phase at Stromboli, a mass flux of at least 10^6 kg/s is required [Fig. 3.9b]. Therefore the Bernoulli process cannot be a major contributor to the pressure drops associated with the underlying phase (or any other seismic phases) related to eruptions at vent 1.

Indeed the Bernoulli process is more significant for low density gas than for the much higher density magma, which at first seems contradictory [3-24]. This is shown in Fig. 3.10 where a maximum mass flux of 1000 kg/s is assumed, and the dynamic pressure is calculated for both a gas (speed assumed to be 100 m/s) and magma (density assumed to be 2500 kg/m^3). The reason for this unexpected behaviour is that though the dynamic pressure is proportional to density, it is also proportional to speed squared [3-24], and speed is related to the inverse square of density by 3-25.

If the modelling had been applied to short-period 'explosion quakes' smaller pressure changes would have been estimated. This is because explosion quakes are just the high frequency part of the much larger broadband eruption signal.

FIGURE 3.9

Fluid speed and mass flux curves

FIGURE 3.10

Bernoulli for gas and magma.

3.4 Source types

3.4.1 Choosing the right source type

In volcano seismology it is common to treat the seismic source as a point source [e.g. *Mariotti et al.,* 1976; *Braun and Ripepe*, 1993; *Ereditato and Luongo*, 1997], just as it is in exploration seismology and global seismology. As already seen, this is not necessarily valid, because seismometers usually need to be very close to a volcano in order to record volcanic earthquakes with good signal to noise resolution. The conditions under which it is reasonable to assume a point source must be investigated.

What about other source types? In the previous section line sources were examined, which can be used to represent a uniform pressure change along a section of conduit. But this is another type of stationary source. A volcano transports magma and gas from deep in the earth to the surface, and therefore, cannot be described without this concept of movement. So why all this emphasis on stationary sources? The reason is because they are relatively simple to work with. However they are too restrictive for volcano seismology. So *moving* sources must be considered also. Consider two types of moving source:

1. Moving point source: wavefronts are produced at one point at any particular time, but that point changes with time.

2. Expanding line source: wavefronts are produced along an entire section of conduit at any particular time, but that length of the conduit section is increasing with time.

Combining these with the two previous source types, stationary point source and line source, there are now four source types [Fig. 3.11]. These source types are defined in terms of fluid pressure changes in the magmatic system. The wavefronts produced by these different sources are shown in Fig. 3.12. Examples are given to show why each is relevant for volcanoes. These four source types are believed to be exhaustive for modelling the possible source of very-long-period and deformation signals.

Point source

The point source is the simplest source type, and implies that fluid pressure is changing at one point only. Broadband recordings demonstrate that the source at Stromboli is isotropic so only purely explosive (or implosive) point sources are considered. If attenuation and the free surface effect are ignored the recorded waveform will match the variation in source pressure except for a travel time delay. A point source will produce concentric spherical wavefronts if the medium is isotropic.

Examples of processes which can be modelled by a stationary point source (or spherical source) are:

- Explosive degassing (magma explosively releases volatiles due to rapid decompression).
- Bubble burst (when bubbles reach the top of the magma column).
- The large dynamic pressure resulting from flow through a narrow conduit section.
- Pressurisation of a spherical magma chamber.

Line source

A line source can be used to represent pressure changing simultaneously throughout a section of conduit. The waveform recorded at each station will match the source signature. Interference produces cylindrical wavefronts [Fig. 3.12d] except at ends of source, where weaker spherical wavefronts result. Particle motion will point perpendicular to the source axis for a very long source. An example of such a source is the pressure rise within a sealed section of conduit due to rising bubbles (advective overpressure) [Fig. 3.12b] proposed by *Sahagian and Proussevitch* [1992].

In reality pressure changes (except shocks) are communicated at the speed of sound, so in order to apply a line source model, the time for a sound wave to travel the length of the conduit section of interest must be small compared to the period of the waves considered.

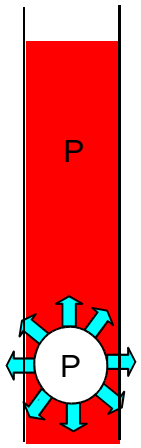

(a) Point source - e.g. explosive degassing

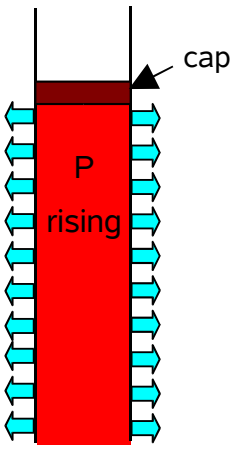

(b) Line source - e.g. pressure rising beneath a cap

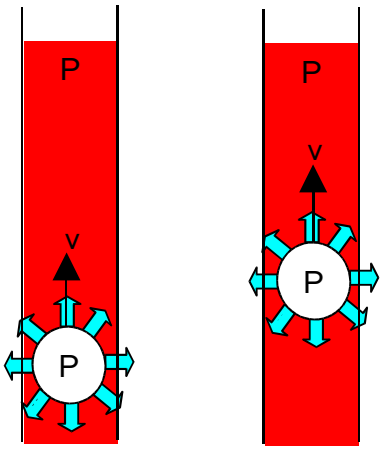

(c) Moving Point source - e.g. rising slug

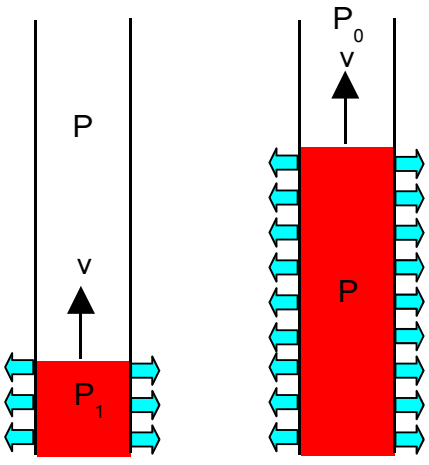

(d) Expanding Line source - e.g. rising magma

Figure 3.11: Four types of source are considered (a) Point source (b) Line source (c) Moving point source and (d) Expanding line source. Pressure forces (blue arrows) are shown. For rising magma, viscous forces are directed in the opposite direction to the velocity of the fluid.

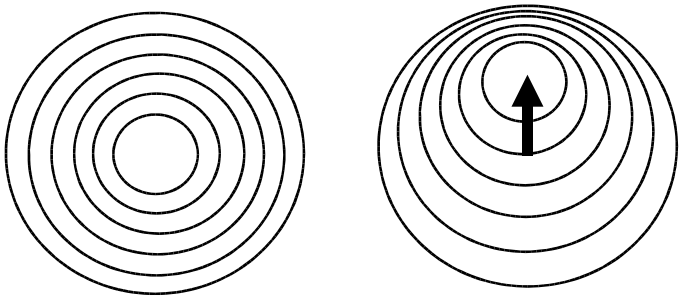

(a) point source, $v=0$ (b) subsonic moving point source, $v<\alpha$

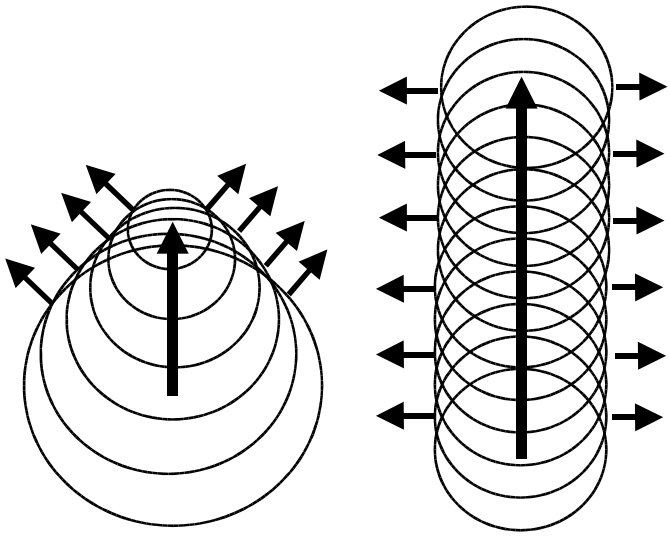

(c) supersonic moving point source, $v>\alpha$ (d) line source, $v=\infty$

Figure 3.12: Wavefronts radiated by different source types. (a) A point source generates spherical wavefronts which are concentric. (b) If a point source moves with a speed, v, less than the p-wave speed in rock, α, spherical wavefronts are generated, but these are no longer concentric, so polarization of signal changes with time. (c) If a point source moves at speed $v>\alpha$ then conical wavefronts are generated (due to interference between spherical wavefronts) – the angle of the cone becomes more acute as v/α increases. (d) A line source generates cylindrical wavefronts, except at the ends where spherical wavefronts are produced. An expanding line source produces the same pattern of wavefronts, except that the source region itself expands at some speed.

Moving point source

A moving point source is used to model a pressure change that moves with time. Moving sources can generate complicated waveforms because the distance between source and seismometer is constantly changing. Each seismometer will record a different waveform. Even if the source is radially symmetric it will not appear to be so. Wavefronts can be non-concentric spheres or cones [Fig. 3.12b,c]. This depends on the source speed compared to the P wave speed in rock:

- If the source speed is less than the P wave speed in rock, the wavefronts are non-concentric spheres (subsonic moving point source). The particle motion vector will swing in the direction of source movement.

- If the source speed is greater than the P wave speed in rock, the wavefronts interfere and produce a conical shock front (supersonic moving point source). If the source is moving up a conduit [Fig. 3.12c] the particle motion vector will get closer to the horizontal as the speed of the source increases. Supersonic moving point sources are not likely at a volcano, because magma, gas, and even pressure waves in the fluid move an order of magnitude slower than the seismic velocity in the surrounding solid.

Examples of moving point sources are: (1) a large bubble or slug rising in a conduit, (2) a rising magma which is overpressurised (compared to the surrounding rock).

Expanding line source

An expanding line source can be used to represent pressure changing along a section of conduit, but new parts of the conduit come under the influence of the changing pressure as time increases. An example of this type of source is the pressure gradient [Table 3.2] in a magma column as the column rises up a conduit. The pressure at all points below the surface of the magma is increasing at the same rate, but because the magma is rising the source region is expanding.

Point source	Line source	Moving point source	Expanding line source
• Bubble burst • Explosive degassing	• Pressure rise throughout a conduit • Shock wave	• Rising bubble • Overpressure term for rising fluid • Shear stress term for rising magma • Bernoulli process for rising fluid	• Pressure gradient term for rising magma

Table 3.2: Classification of source types. Each of the volcanic processes categorised here acts as an azimuthally isotropic source, and is therefore a candidate for the source of VLP signals at Stromboli. A combination of a moving point source and an expanding line source is required to model magma rise. This applies whether the magma rises at a constant speed, or varies as in stick-slip models [*Denlinger and Hoblitt*, 1999].

3.4.2 Wrong source experiment

In order to demonstrate how important it is to select the correct source type, the following test was conducted. A moving point source, rising at speeds, v, from 0 m/s (point source) to infinity (line source), was simulated in order to generate synthetic travel-time data for the 1992 seismic array deployed by Leeds University. These travel-time data were inverted for location (by reduction of least squares), assuming a stationary point source. The aim of this experiment was to investigate whether a moving point source is consistent with very-long-period (VLP) phases at Stromboli.

To generate these synthetic travel-time data a program was written. The input parameters were the upper and lower depths of the conduit (assumed to lie

vertically below the crater region) and the rise speed of the source. At time, *t=0,* the source starts to rise from the base of the conduit. The program calculated the time at which the *maximum amplitude* signal (not the first arrival) arrives at each of the positions occupied by stations in the 1992 experiment. This was done because these VLP phases have emergent onsets, and so first onsets cannot be picked from real data. The maximum amplitude corresponds to the position when the source is at its closest approach to each station because the source function assumed is a delta pulse. Several speeds for the P wave velocity in rock were used, from 1200 m/s to 2000 m/s.

The estimated source location was found to depend strongly on *v*. This is not surprising since at low rise speeds the source acts like a stationary point source, whilst at high rise speeds the source acts like a line source. The estimated source location becomes more inaccurate as the speed of the moving source decreases [Fig. 3.13]. This is because for lower source rise speeds, the differential travel-times between different stations increase, and it becomes harder to find a point source location consistent with the synthetic travel-time data. The main results are:

- Estimated source locations all lie on the opposite side of the actual source region from the seismic array. This is an artifact of the array constellation which lies on one side of the source region [e.g. *Lilwall and Francis*, 1978].

- For source regions which extend from a depth of 600-700 m, and up to the crater region, there is no convergence for source speeds less than half the speed of P waves in the rock.

Since *Luckett* [1997] assumed a point source, and got his data to converge to a location 600-700 m below the vents, the last bullet point above suggests that the source of these VLP phases is either:

1. a point source, or

2. a moving point source which rises faster than 850 m/s (if P wave speed in the rock is assumed to be 1700 m/s).

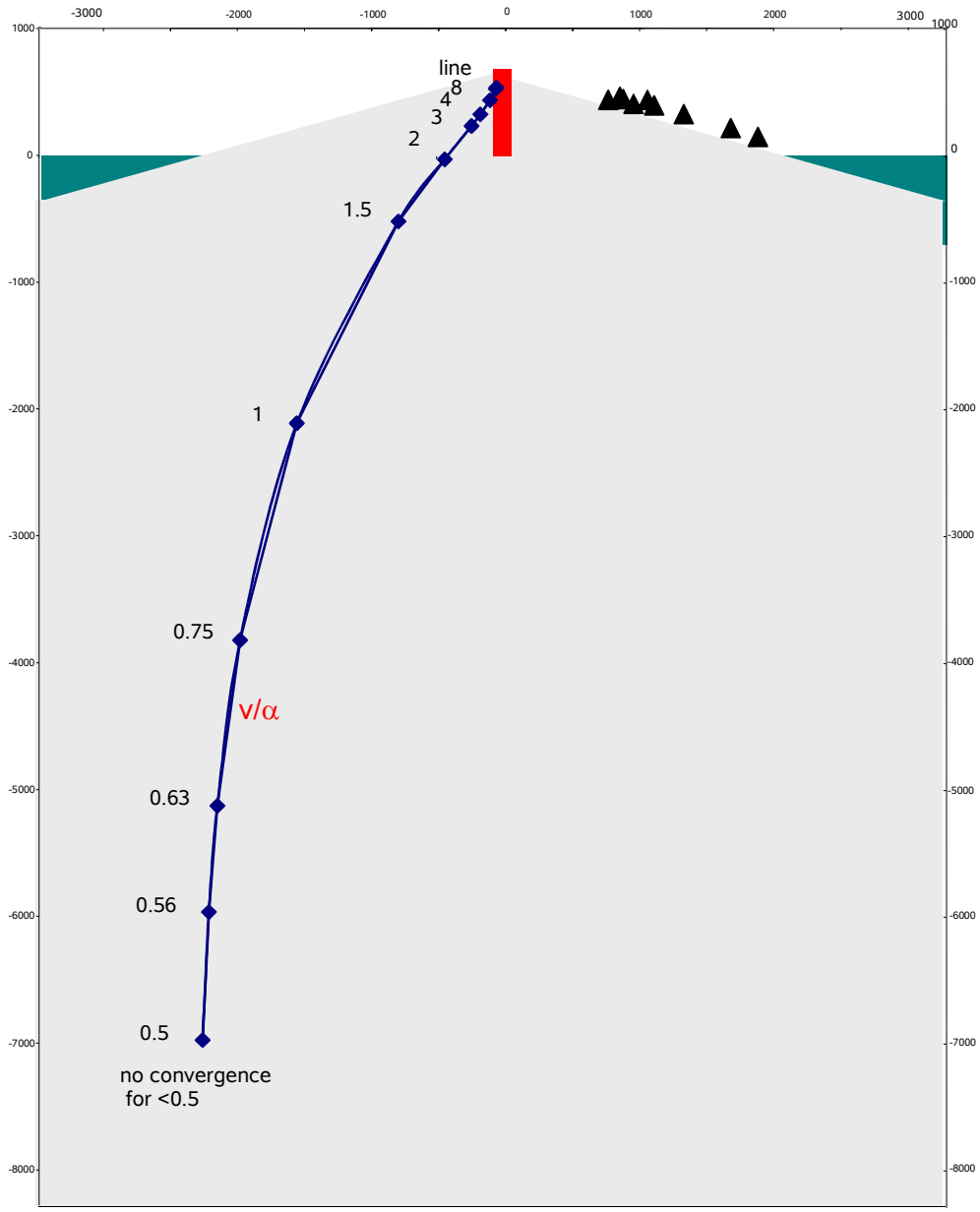

Figure 3.13: This demonstration shows what happens if the source is assumed to be a point source, when in fact it is a moving source. Stations used (black triangles) correspond to the Leeds 1992 array. A point source, moving from (0,0) to (0,700) was used to generate travel time data corresponding to the arrival of the maximum signal at each station. Travel-time data were inverted using a least-squares algorithm to find the source location. This was done for a range of different source rise speeds (v), and a range of different P wave speeds in the rock (α).

Solutions were found to depend on the ratio v/α None of the solutions fall within the actual source region (the conduit, marked by the red box). Values of $v/\alpha > 2$ lead to reasonable solutions, but solutions deteriorate rapidly as v/α decreases. No convergence was found for v/α below 0.5.

If it were neither of these, *Luckett* [1997] wouldn't have got the data to converge. Closer analysis of Fig. 3.13 reveals that a speed of more than 3400 m/s is required for a moving source, otherwise *Luckett* would have concluded the source was located at great depth, far on the other side of the conduit from the seismic array. Even shock fronts are unlikely to approach anything near this speed in the conduit. The inescapable conclusion is that these VLP phases are due to a (stationary) point source.

For moving and/or extended sources above sea level, and greater than 200 m in extent, inversion assuming a point source fails. Again, since *Luckett* [1997] did achieve a solution, the implication is that extended sources of more than 200 m in extent are not consistent with the VLP phases. Anything smaller than this can be treated as a point source anyway.

3.5 Conclusions

It is not trivial to calculate pressure in the volcano from seismic data, because:

1. The source may not be a point source.
2. Near field terms must be considered in addition to far field terms, and these decay differently.
3. Waves are subject to many other processes in addition to geometrical decay, as they interact with the conduit wall, rock and the free surface.

For VLP phases some effects are even more pronounced (e.g. near field effects, tilt) whereas others aren't so important (e.g. stratigraphy, attenuation).

In this chapter a new modelling technique was derived for calculating pressure based on extrapolating the displacement recorded on seismograms back to conduit wall using decay laws, and then using Hooke's Law to estimate the pressure change. The decay laws used took into account near and far field terms. Separate techniques were developed for a point source and a line source, though the methods followed the same lines. These techniques were applied to the underlying phase corresponding to eruptions at vent 1, which had an amplitude of ~20 μm at station 197.

Results for a point source showed that:

- Source radii of less than 40 m are not possible because the radial strain would exceed 10^{-3}.
- For a conduit radius of 40 m, a pressure change of 4 MPa is required.
- For a magma chamber with a radius of 100 m, a pressure change of 0.5 MPa would suffice, which corresponds to a radial strain of ~10^{-4}.

Results for line source showed that:

- Radial strain is below 10^{-3} for conduit radii greater than 4 m
- For a conduit radius of 4 m, a pressure change of 3 MPa is required
- For a conduit radius of 10 m, a pressure change of 0.5 MPa will suffice, which corresponds to a radial strain of ~10^{-4}.

Results also showed that the Bernoulli effect cannot account for VLP phases at Stromboli, because the mass flux required greatly exceeds 1000 kg/s which is the maximum value observed during normal eruptive activity at Stromboli.

Inversion of synthetic travel time data generated by a moving source, but assuming a point source, suggests VLP phases originate from a point source. However, rather than assume this result is correct it will be verified by other techniques in this thesis.